ISR-MA/rh

28th November 1974

ISR PERFORMANCE REPORT

Run 554 - 22 November 1974

Rings 1 and 2 - 26 GeV/c - Booster

Fourth test of steel low-β section

Conclusions

The closed orbit was corrected successfully. The results show the effect of increasing the central orbit distortion in order to correct the "sextupole" contribution on the outer orbits. The final corrections are in file LO26.

The bump file LOB1 was measured in Ring 1 in I4. On central orbit the bump was 2 % too large. Between central orbit and +20 mm, the bump height changed by 5.3 % which gives a far stronger radial dependence than occurs in the normal machine. The I7 monitor was also calibrated.

The working lines in both rings were shifted beyond the 7 Q_v = 62 resonance. All four substacks were measured and corrected in both rings. These corrections are stored in the button files LOW1 for Ring 1 and LOW2 for Ring 2.

Final stacks of 24.76 A in Ring 1 and 25.73 A in Ring 2 were made with a luminosity of 22 $\mu b^{-1} s^{-1}$ in I7. The initial decay rate in Ring 2 was 18 ppm/min. A slowly growing pressure bump in I4 made it necessary to scrape 2 A from Ring 2. As there was no time left, the beams were then dumped.

It appears that it is only possible to work for 15 to 20 minutes at the 25 A current level before the I4 vacuum becomes critical.

Closed orbit corrections (G. Guignard)

Two problems were looked at:

i) whether localized sextupoles contributed an appreciable distortion to the off-axis orbits;

ii) what is the best procedure for correction taking into account the above factor and the proximity of the Q = 9 integer resonances.

CI26 was used as a starting point in Ring 1. All measurements made in this ring are listed in Table 1. As can be seen, the initial orbits are quite good and we did not correct the vertical plane further. For the horizontal orbit, we used the CØCØ program for correcting on the centre line. This worked well on the centre line, but the distortion increased on the extreme orbits. To balance these distortions across the aperture, we then corrected at injection. The final results show how the sextupole distortion can be transferred to the central orbit where it is of less importance. It can also be seen that the increased proximity of the integer resonance makes this distortion far more evident at +40 mm than at -40 mm.

In Ring 2 we started by switching all H and CR magnets off. Under normal conditions, this is a standard procedure. The distortion was minimum at injection (as would be expected), but it was not possible to accelerate beyond +10 mm. We then corrected both planes at +10 mm using the CØCØ program (see Table 2). The horizontal correction was satisfactory (obtained p-to-p 6.2, expected p-to-p 4), but the vertical was not so efficient (obtained p-to-p 14, expected p-to-p 6). This could be due to the program being sensitive to Q-values close to 9 (since sin (πQ) tends to zero). This correction was repeated in both planes in order to balance the multipole contribution across the aperture and to improve further the vertical orbit. We were successful in the vertical plane, but less so in the horizontal plane. The injection orbit was over-corrected and the top orbit correspondingly under-corrected. Lack of time prevented us making more corrections. The corrections for both Ring 1 and Ring 2 were put in the file L026.

We note from the results in Tables 1 and 2 that:

- In both rings, the extreme orbits could be improved at the expense of the central orbit, i.e. the sextupole contributions are quite strong.

- The basic dipole distortion is dominant, as can be seen in Ring 2 when all CR and H-magnets were switched off.
- The normal 'CI' corrections give quite good results but can be considerably improved horizontally.
- Nevertheless, the procedure appears to be quicker starting from a standard orbit correction rather than from the uncorrected machine, since the CØCØ program appears to be less efficient with these Q-values.
- Corrections can be made at first on the centre line and then, the sextupole contribution can be re-distributed across the aperture by correcting at injection (so avoiding the high Q-values at +40 mm).

TABLE 1

Closed orbit measurements with the steel low-β section at different correction stages in R1

Conditions of measurement or actions taken	Average position (mm)	p-to-p H (mm)	p-to-p V (mm)
CI26 created on FP	0.3	11.1	5.2
on-line correction in H-plane at centre line			
after this H correction	-37.1	8.8	4.6
	0.3	4.7	4.9
	41.4	15.8	8.9
on-line correction in H-plane at injection			
after this 2nd correction	-37.1	4.4	4.6
	- 0.5	11.4	5.2
	41.7	8.7	10.5

TABLE 2

Closed orbit measurements with the steel low-β section at different correction stages in R2

Conditions of measurement or actions taken	Average position (mm)	p-to-p H (mm)	p-to-p V (mm)
H, CR magnets OFF	-37.4 - 0.9 10.7	16.2 26.1 30.4	13.2 20.0 23.3
on-line correction in both planes at +10 mm after these corrections	-37.6 - 0.6 42.0	12.2 5.3 21.7	13.0 14.4 13.5
on-line correction in both planes at injection after these corrections	-37.6 0.1 42.5	5.6 22.8 18.8	6.0 4.6 5.4

Monitor and bump calibrations (K. Potter)

A measurement of the Ring 1 bump was made with the I7 scraper in order to check the effect of the Q-shift. A 2 mm displacement made with the program LUMS (bump file LOB1) was measured at central orbit and at r = +20 mm. The results are shown in Table 3. The bump was found to be 2 % too large on central orbit (the same error as found in Run 543), but this was considered to be negligible for present purposes since known hysteresis effects are of the same order. At +20 mm, the displacement was 5.3 % smaller indicating a much stronger dependence on radial position than in the normal machine. This requires further investigation together with a proper calibration of the bumps before the low-β insertion is used for physics experiments. From the measurements at zero displacement, a median plane tilt of 5 mrad is indicated, which is not larger than normal.

The I7 luminosity monitor was then calibrated in the normal way but displacing beam 1 only, since in Ring 2 the bumps have not yet been calibrated. Beams of 4 A stacked around central orbit were used. The monitor constant was found to be 4.63 mb and the beams used for the calibration had an h_{eff} = 1.30 mm. A final position of +0.34 mm was chosen for Ring 1 to give the optimum luminosity.

TABLE 3

Results of the bump measurements in R1 in I7 using the LOB1 bump file (26 GeV/c, low-β)

Radial position	Z_{set}	Z_{meas}	$Z_{meas} - Z_{set}$	"Error"
	mm	mm	mm	
Central orbit	0	-14.18×10^{-2}	-14.18×10^{-2}	+2.2 %
Central orbit	+2	190.19×10^{-2}	-9.81×10^{-2}	
+20 mm	0	-3.47×10^{-2}	-3.47×10^{-2}	-3.1 %
+20 mm	+2	190.43×10^{-2}	-9.57×10^{-2}	

Tilt of median plane = 5.4 mrad

Radial dependence of bump = 5.3 % over 20 mm
(cf. 1 % for FP line at 22 GeV/c)

Working lines (P.J. Bryant)

The baselines used in the previous low-β runs (file LB2) was shifted so that the full stacking aperture was beyond the 7 Q_v = 62 resonance (new baseline file LB5). This was done prior to the closed orbit correction and the bump calibrations. Figure 1 shows the Ring 2 baseline and the position in the Q-diagram relative to the probable safe limit of the feedback system, the resonances and the old line (LB2). There were two unexpected features:

i) Ring 1 and Ring 2 behaved identically except Ring 2 required a further shift of ΔQ_v = -0.007 when changing the working lines.

ii) The standard B-pulse of 12'500 gave injection orbits at -36 and -37 mm (can this be a modification of $\alpha_{p,average}$ by the low-β insertion?). The B-pulse was changed to 12'475 giving injection at -39 and -40 mm.

Space charge post-stresses in Ring 1 (K. Hübner, K. Brand)

i) First stack for measuring post-stresses

The working line was measured at the beginning and after each sub-stack. Figures 2 and 3 give the results. Since the empty buckets used by the Q-diagram meter filled up on their way through the stack, the Q-values at the top of larger stacks could not be measured. The final stack had only 21 A due to the current loss in the Q-scans. If one takes into account the Q-shift due to this beam loss, the measured part of the working line agrees with the theoretical line. However, the Schottky scan taken at the end, shown at the bottom of Figure 3, indicates that the top of the stack had crossed the diagonal. In this context, a loss of 0.6 A during the application of the last post-stress has to be mentioned. The parameters of the post-stresses (1, 2, 3, 4) are given in Appendix I.

ii) Second stack

Four substacks were made with post-stresses 1, 2, 3. We noticed a vertical blow-up at the top visible on the BP-monitor. It may be due to an accidental crossing of $2\,Q_h - Q_v = 9$ by one of the substacks. The last post - stress (No. 4) was not applied. A Schottky scan was taken. It is shown in Figure 4.a. The decay rate was in the 10^{-4} min^{-1} range, which may be due to the 7th order resonance. A Q-correction was performed which is shown as post-stress No.5 in Appendix I. The resulting Q-values are given in Figures 4.b and 4.c.

It is apparent from Figure 4.b that the stack was out of 7th order resonances. Before we could observe the decay rate in this new position, a pressure bump occurred in I4. Scraping in Ring 2 removed the Ring 1 pressure bump, but then no time was left. Figure 4.c gives the result of the Q-scan performed before the dumping of the beam. The horizontal

measurement confirms the Schottky scan whereas the vertical one does not mean much. There was no time left for a decay rate measurement.

Space charge post-stresses in Ring 2 (P.J. Bryant)

i) First stack for measuring post-stresses

Figure 5 gives the Q-diagram meter scans after correction for each substack. The final post-stresses and the RF parameters used are listed in Appendix II. These post-stresses and those for Ring 1 are stored in the button files LOW1 (Ring 1) and LOW2 (Ring 2).

ii) Second stack

Using the post-stresses in Appendix II, a second stack was made. Stacking was continued after the fourth post-stress to 25.73 A. The decay rate was 18 ppm/min. Spillout was high and the stack was frequently scraped during stacking.

Schottky scans were made and Q-corrections applied. The decay rate, however, increased to 100 - 200 ppm/min. and a further Schottky scan showed some discrepancies in the expected Q-shifts. 2 A then had to be scraped away to stabilize the vacuum. It is very likely that the Schottky scans were influenced by neutralization Q-shifts and the decay rates were undoubtedly affected by the pressure bump. The Q-diagram scans of the first stack, however, were taken under good vacuum conditions, so there is no reason to modify them. On the Schottky scans taken in Ring 2, 9 Q_v = 80 could just be identified.

Vacuum observations (O. Gröbner)

Final stacks of 24.7 A in Ring 1 and 25.7 A in Ring 2 were obtained at 01.40 h. During the stacking of the last substack, gauges near the beam dump of Ring 1 (269.4) and near the inflector of Ring 2 (248.6) showed a pressure increase in the 10^{-10} torr range. The pressure indicated by these gauges decayed quite rapidly once stacking was stopped.

Two further pressure rises to about 1×10^{-10} torr could be observed at 501.6 (Ring 1) and 860 (Ring 2). Both places were known from previous vacuum limit runs. These pressures remained constant in the presence of the stacks.

Indication of the clearing currents remained stable for both rings until about 02.00 h. Only then the familiar pressure bump in 364 had become noticeable. A time plot of the average pressures (Rings 1 and 2) of octant 4 as measured with the clearing currents is shown in Figure 6. Ring 1 remained stable until about 2.30 h. The increase which started at that time can be attributed to the spreading out of the pressure bump into the intersection I4.

Shortly after 2.30 h, the average pressure in octant 4/Ring 2 exceeded 7×10^{-9} torr and from then onwards, the current signal and the analog scanner were saturated. The highest reading of gauge 364 was about 3×10^{-8} torr before beam 2 was scraped to 23.9 A. The local pressure near 364 must have been considerably higher than the indication of the gauge or the average reading given by the clearing currents. Too little time was left to see whether the scraping was sufficient to establish stable vacuum.

The observation of the pressure rise near 364 is consistant with our earlier observations. To avoid this pressure rise, it seems necessary to limit the beam current in Ring 2 to 22 A (optimistic) or 20 A (realistic).

K. Brand
P.J. Bryant
O. Gröbner
G. Guignard
K. Hübner
S. Pichler
K. Potter

Appendix I. Stacking Parameters and Post-Stresses in Ring 1.

Momentum	26.588 GeV/c	Linear density	0.436 A/mm
Final current	24.0 A	Step-back	6.6 Hz
Stack limits	+40 to -15 mm	Γ	0.5
Substack current	6.0 A	Vfinal	700 V
Substack length	13.75 mm	Degree of shaving	50 mA in final bucket

Sub-stack No.	Post-Stresses in Button File LOW1 Baseline LB5									
	ΔQ_H	ΔQ_V	$\Delta Q'_H$ inner	$\Delta Q'_V$ inner	$\Delta Q'_H$ outer	$\Delta Q'_V$ outer	$\Delta Q''_H$ inner	$\Delta Q''_V$ inner	$\Delta Q''_H$ outer	$\Delta Q''_V$ outer
1	0	.006	0	0	-1.18	0.91	0	0	17.0	-21.2
2	-.005	.005	-.43	0.55	-1.29	1.49	-14.5	18.2	45.5	-56.8
3	-.015	.022	-1.5	1.87	0.88	-1.09	-26.8	33.4	-20.9	26.0
4	-.011	.012	1.5	-1.91	0.44	-0.55	72.5	-90.6	-10.4	13.0
5	0	0.017	0	-0.5	0	-0.5	0	0	0	0

Appendix II. Stacking Parameters and Post-Stresses in Ring 2.

Momentum	26.588 GeV/c	Linear density	0.436 A/mm
Final current	24.0 A	Step-back	5.0 Hz
Stack limits	+40 to -15 mm	Γ	0.5
Substack current	6.0 A	Vfinal	700 V
Substack length	13.75 mm	Degree of shaving	39 mA in final bucket

Sub-stack No.	Post-Stresses in Button File LOW2 Baseline LB5									
	ΔQ_H	ΔQ_V	$\Delta Q'_H$ inner	$\Delta Q'_V$ inner	$\Delta Q'_H$ outer	$\Delta Q'_V$ outer	$\Delta Q''_H$ inner	$\Delta Q''_V$ inner	$\Delta Q''_H$ outer	$\Delta Q''_V$ outer
1	0	0	0	0	-.73	1.54	0	0	0.4	-21.2
2	-.005	.005	-.43	0.55	-1.39	1.74	-14.5	18.2	45.5	-56.8
3	-.015	.022	-1.5	1.87	1.17	-1.09	-26.8	33.4	-20.9	-7.3
4	-.011	.012	1.5	-1.91	0.97	-.55	72.5	-90.6	-10.4	13.0

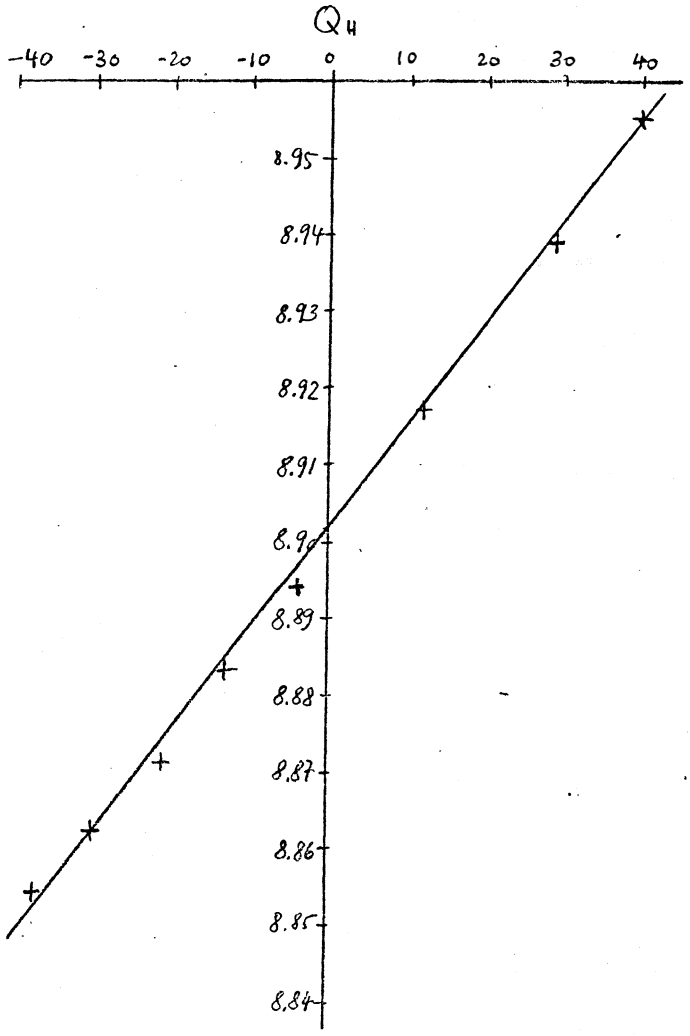

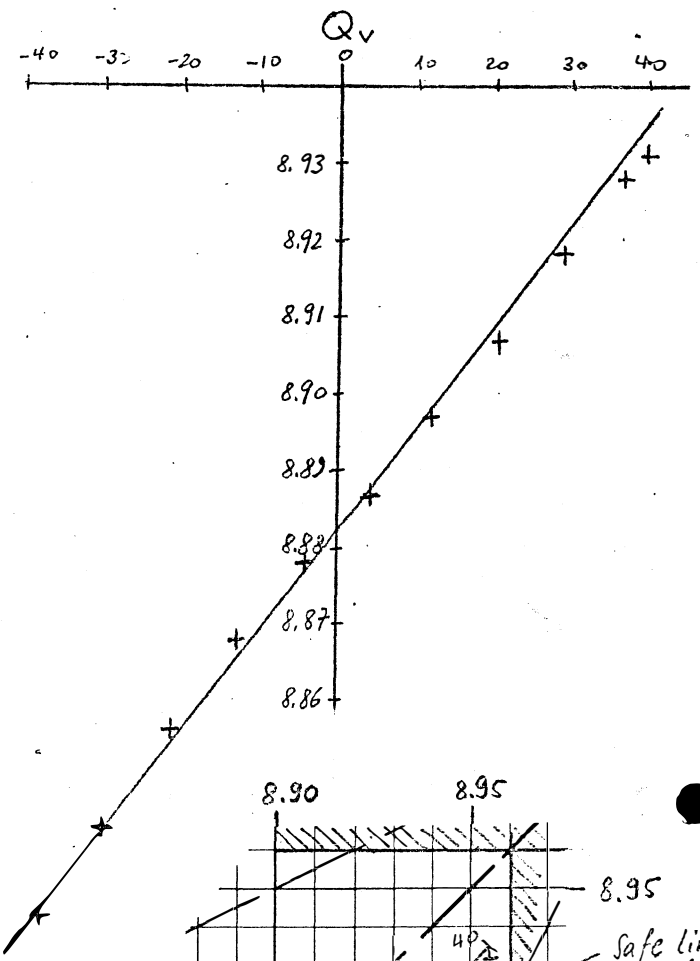

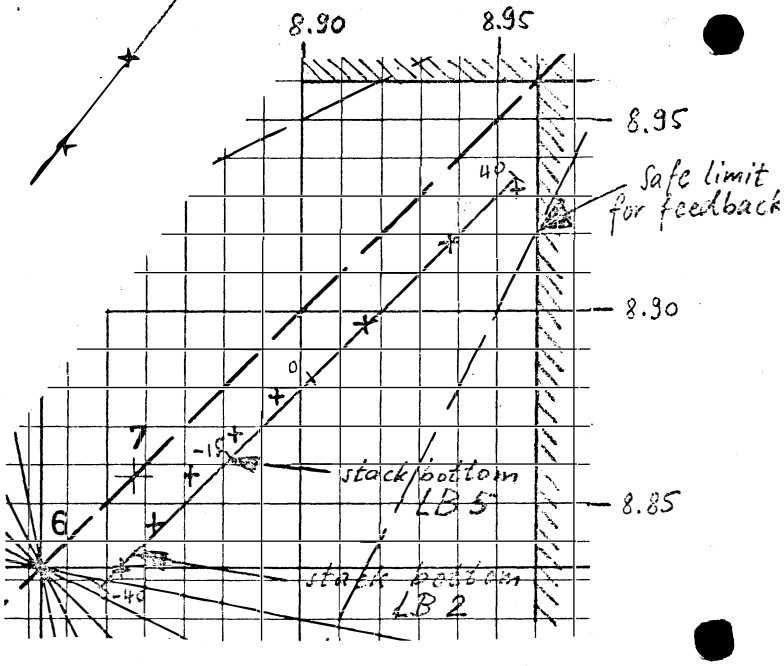

Fig 1 Baseline measurements in R2 and current file LB5 for both rings.

PFW CURRENTS LB 5

1CP	+47.29	1SF	+35.40	1SD	+34.52
2CP	+42.65	2SF	+33.20	2SD	+32.42
2Q1	-1.22				
/PF					
1PFF1	+59.23	1PFF2	+20.24	1PFF3	+8.40
1PFF4	+20.53	1PFF5	+22.05	1PFF6	+21.29
1PFF7	+22.44	1PFF8	+25.29	1PFF9	+28.37
1PFF10	+26.42	1PFF11	+46.53	1PFF12	+40.92
1PFD1	-13.77	1PFD2	-0.39	1PFD3	+7.28
1PFD4	+11.77	1PFD5	+11.72	1PFD6	+10.84
1PFD7	+12.16	1PFD8	+15.82	1PFD9	+18.80
1PFD10	+12.94	1PFD11	+31.96	1PFD12	+28.54
2PFF1	+60.91	2PFF2	+20.97	2PFF3	+8.89
2PFF4	+21.14	2PFF5	+22.63	2PFF6	+21.70
2PFF7	+22.85	2PFF8	+25.66	2PFF9	+28.71
2PFF10	+26.54	2PFF11	+46.75	2PFF12	+40.99
2PFD1	-15.87	2PFD2	-1.34	2PFD3	+6.62
2PFD4	+11.01	2PFD5	+11.01	2PFD6	+10.23
2PFD7	+11.67	2PFD8	+15.26	2PFD9	+18.31
2PFD10	+12.62	2PFD11	+31.64	2PFD12	+28.44

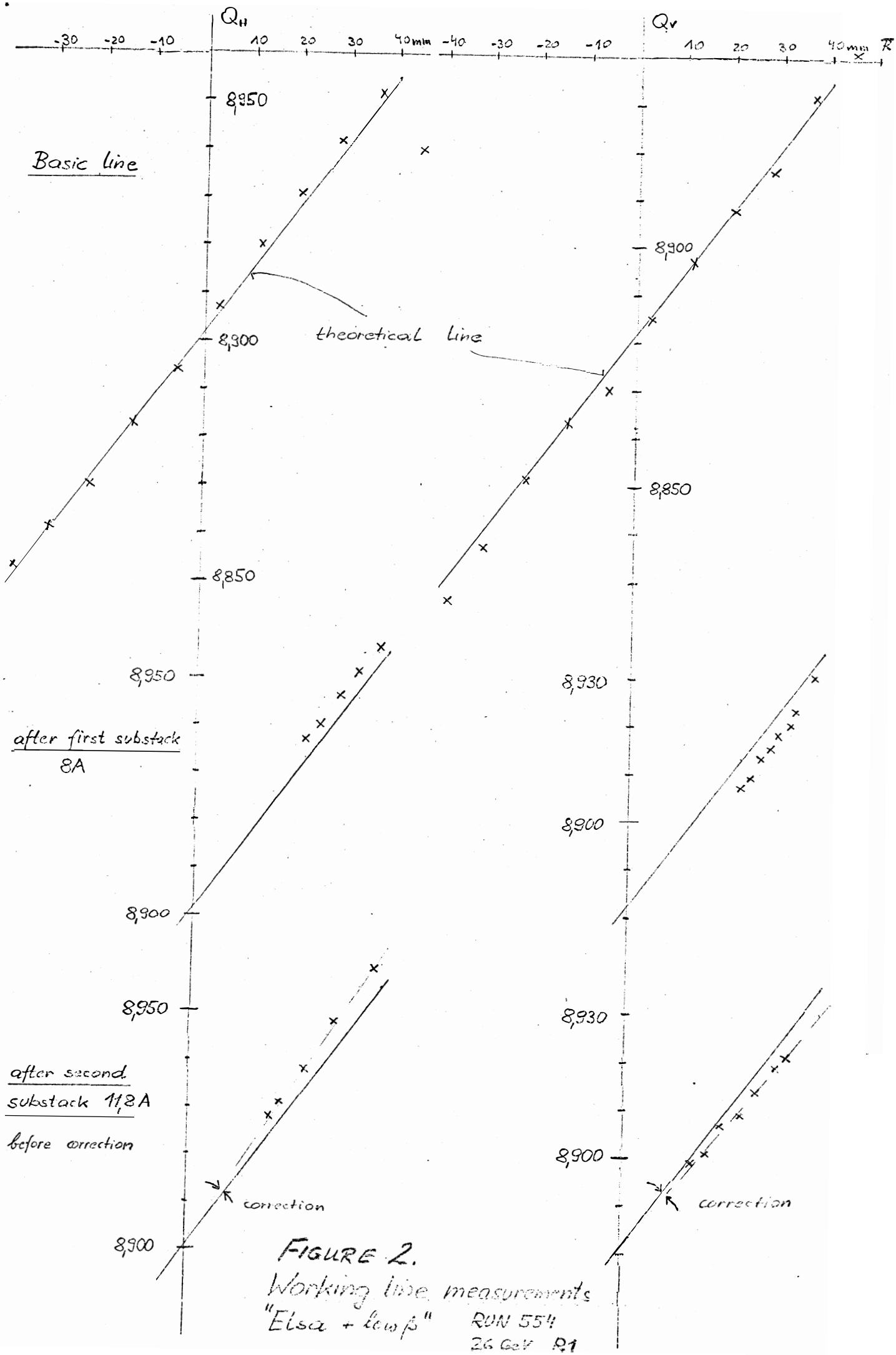

FIGURE 2.
Working line measurements
"Elsa + lamps" RUN 554
26 GeV P1

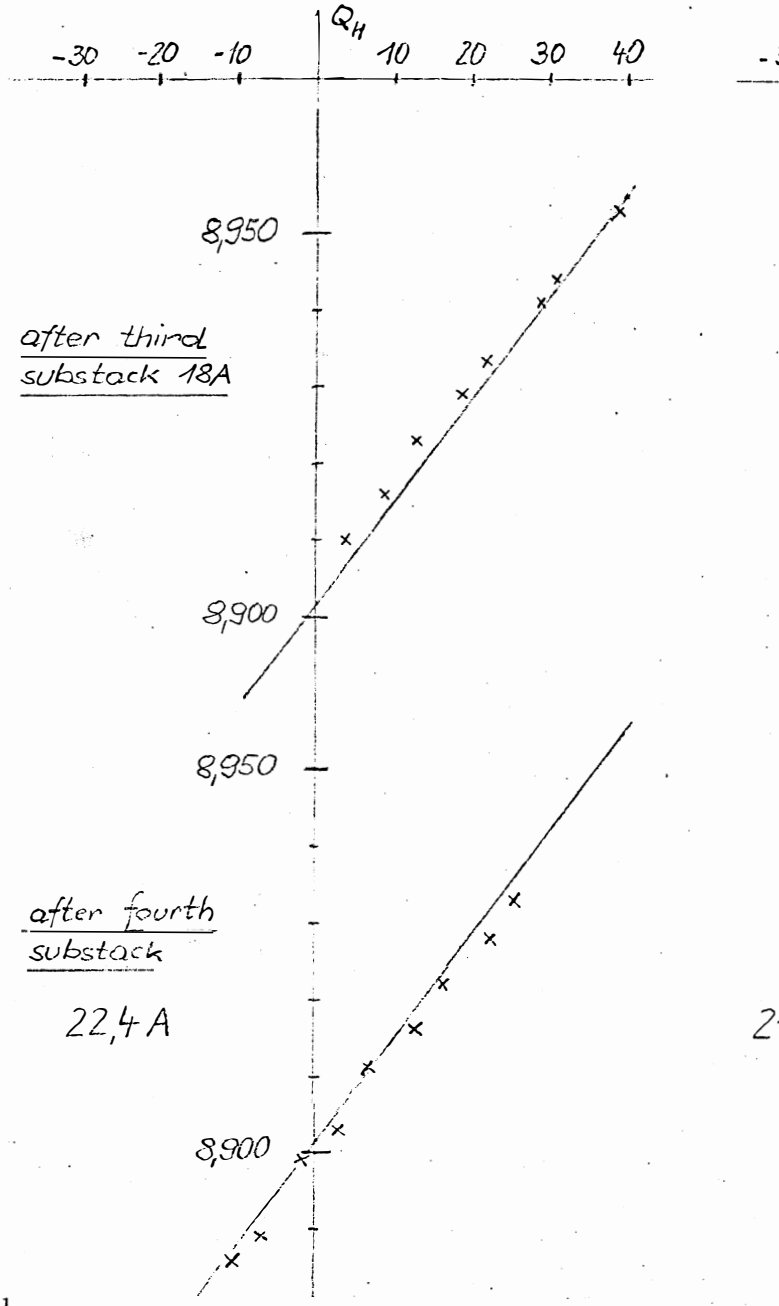

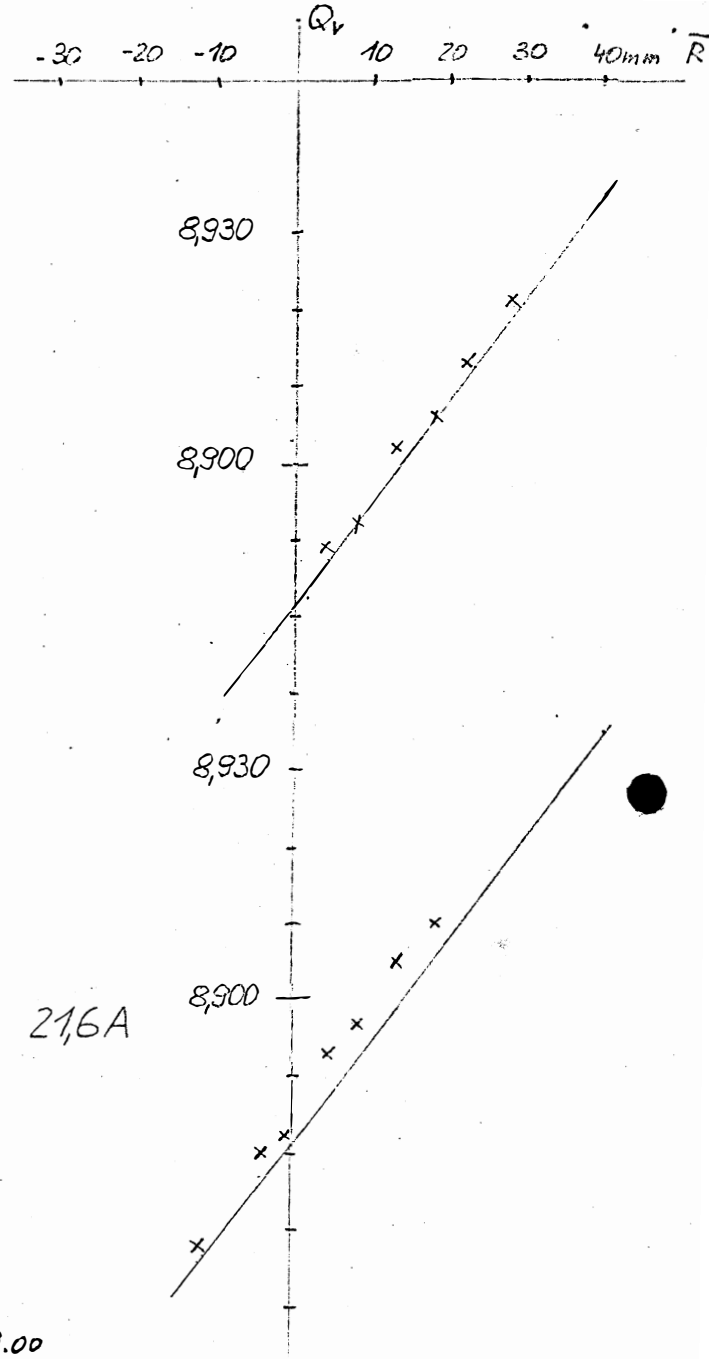

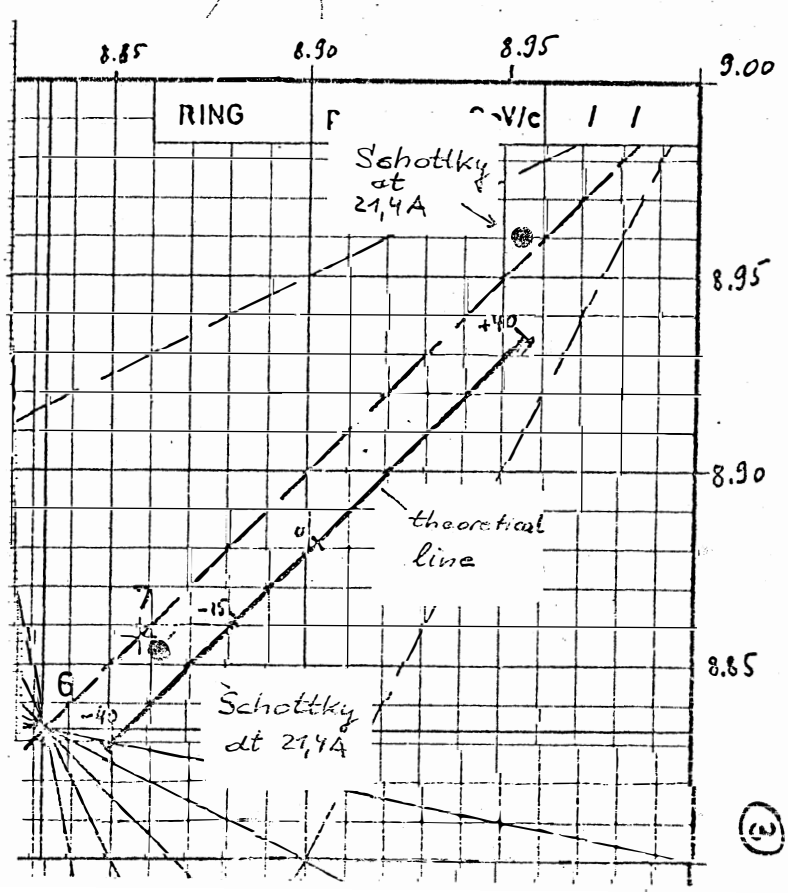

Q-values of stack edges

after fourth substack

Figure 3

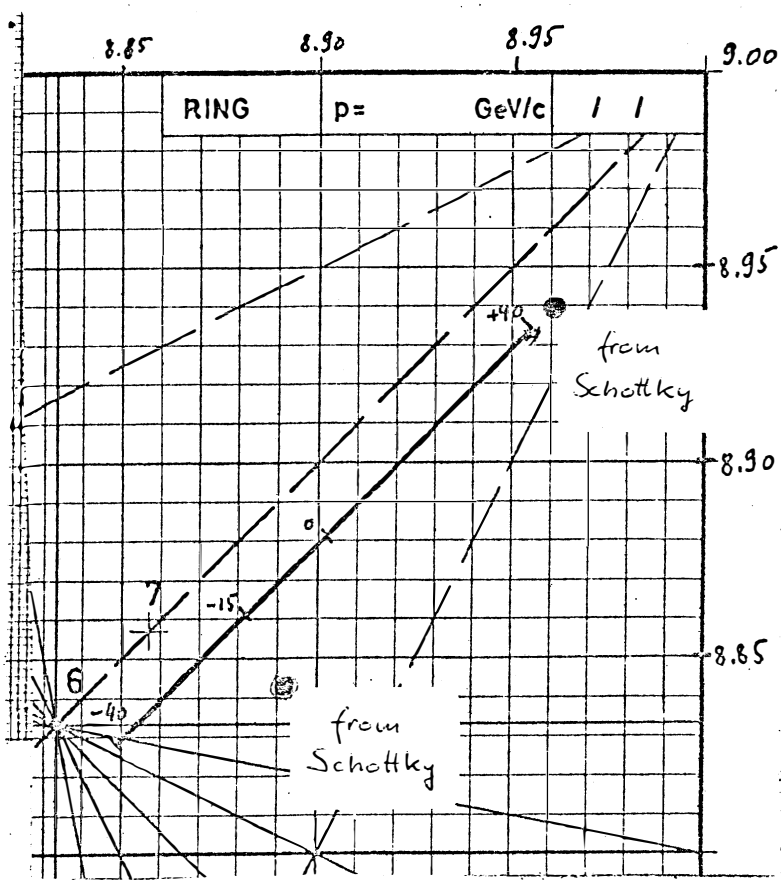

Schottky scan 25A

4th substack with postresses 1,2,3

Fig. 4a

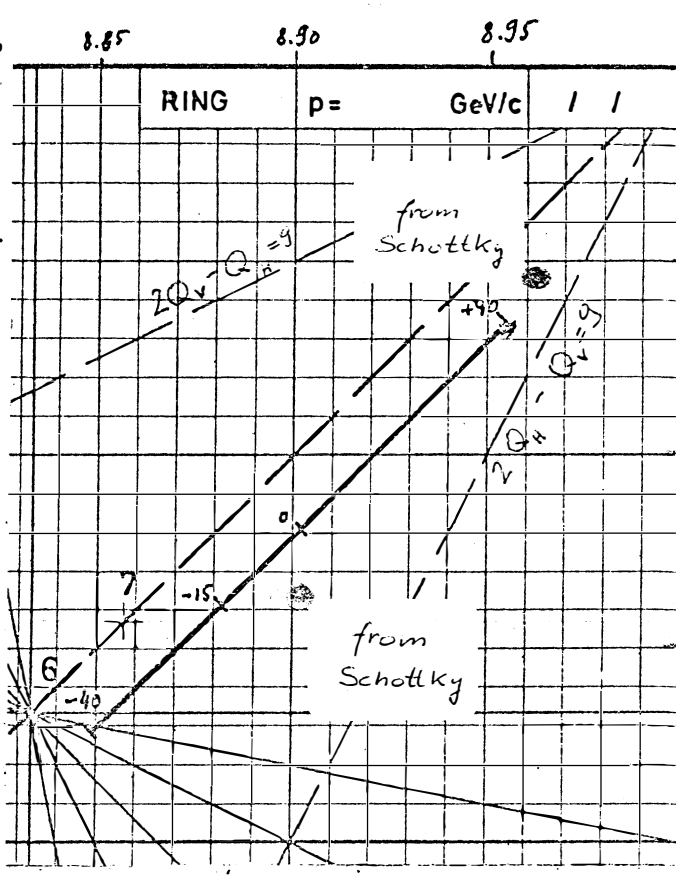

Schottky scan 25A

4th substack with postresses 1,2,3,5

Fig. 4b

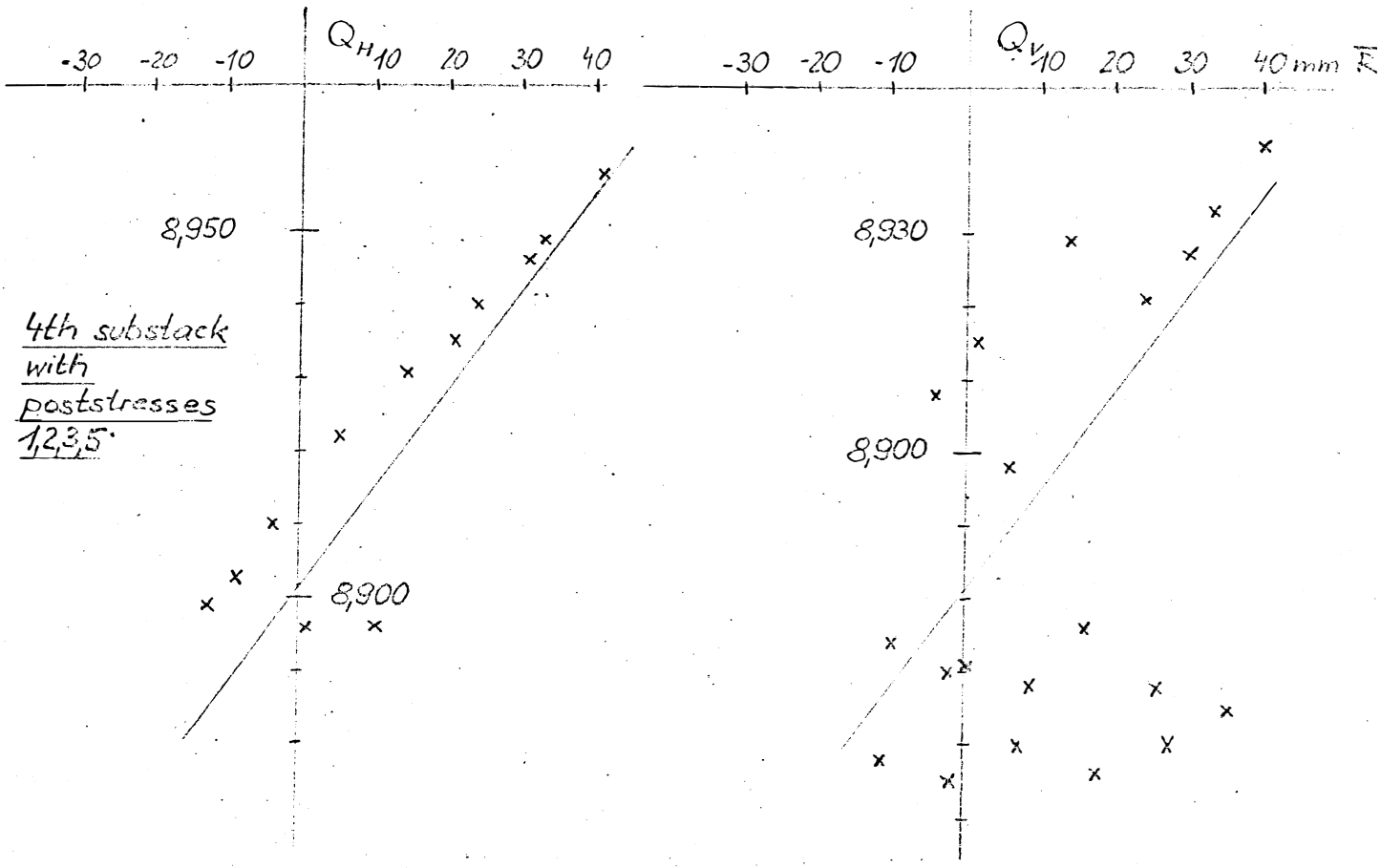

Fig. 4c

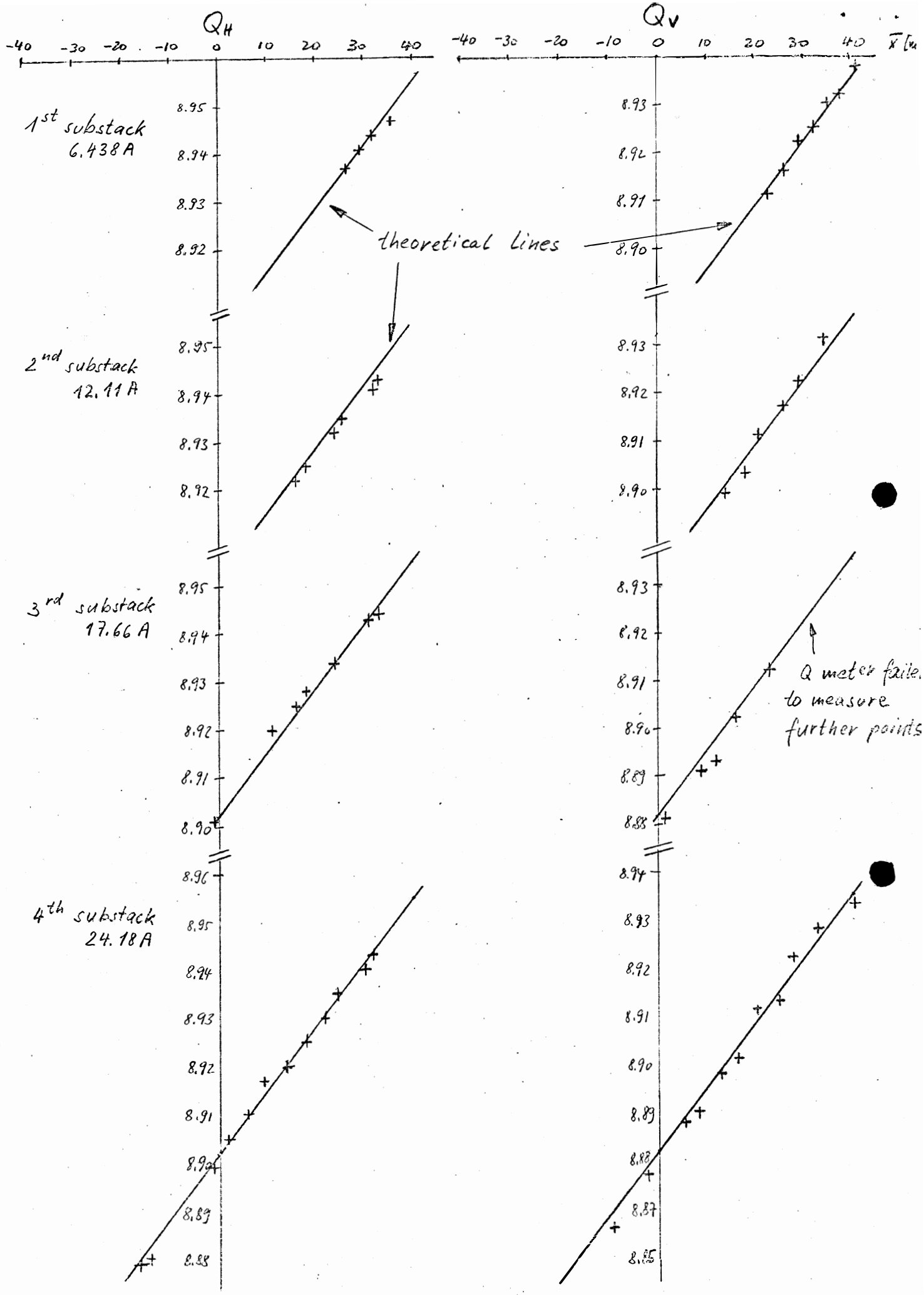

Fig. 5 Q-scans of substacks after correction in Ring 2 at 26 GeV/c with the steel loaf section

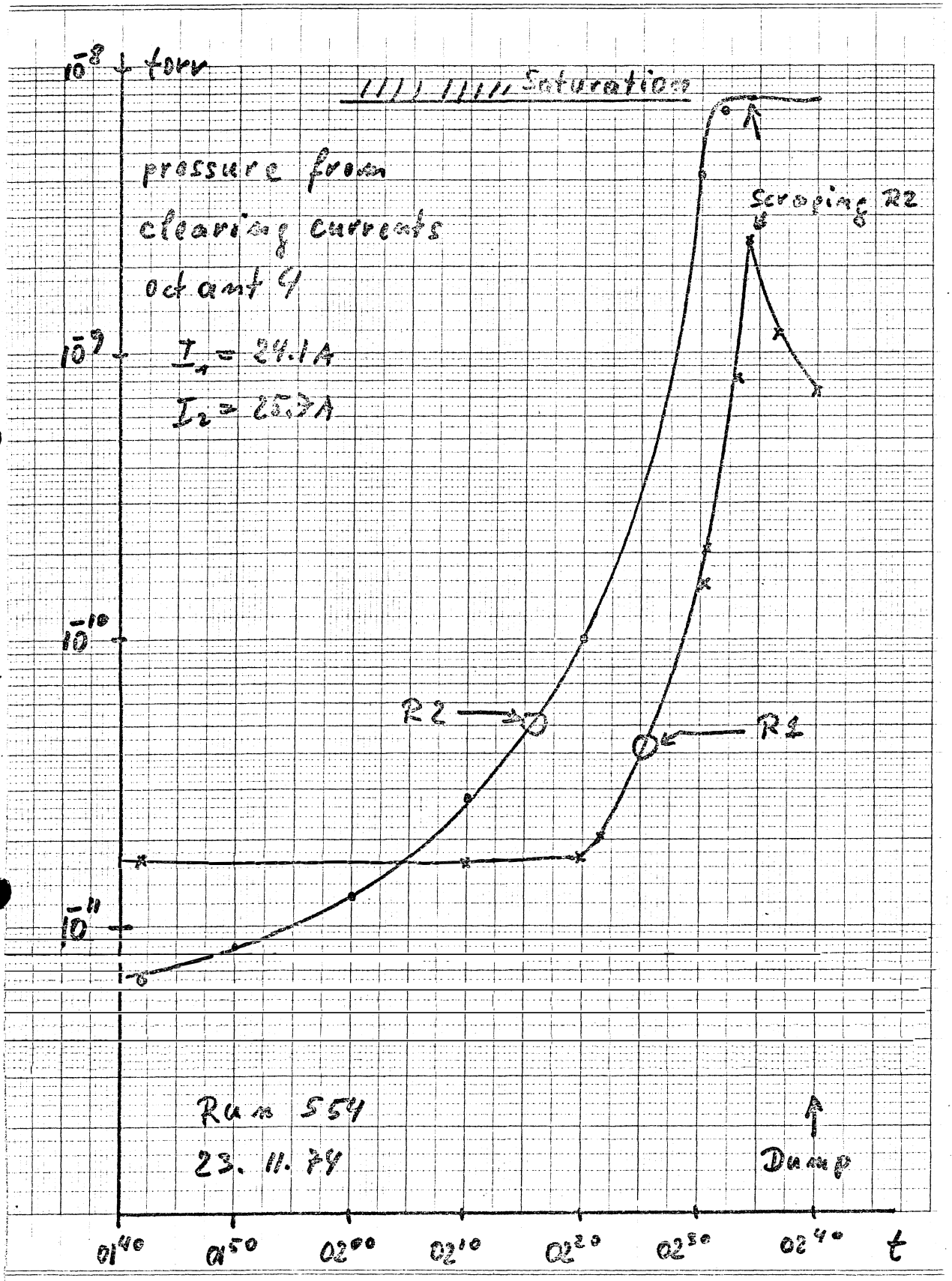

Figure 6

Ed. Aerni-Leuch, Bern, Nr. 525